

Chemical Trend of Superconducting Transition Temperature in Hole-doped CuBO_2 , CuAlO_2 , CuGaO_2 and CuInO_2

Akitaka Nakanishi*, Hiroshi Katayama-Yoshida

Department of Materials of Engineering Science, Osaka University, Toyonaka, Osaka 560-8531, Japan

Abstract

We calculated the superconducting transition temperature T_c of hole-doped CuBO_2 , CuAlO_2 , CuGaO_2 and CuInO_2 using first-principles. The calculated T_c are about 50 K for CuAlO_2 , 10 K for CuBO_2 and CuGaO_2 and 1 K for CuInO_2 at maximum in the optimum hole-doping concentration. The low T_c of CuInO_2 is attributed to the weak electron-phonon interaction caused by the low covalency and heavy atomic mass.

Keywords: A. Semiconductors; C. Delafossite structure; D. Electron-phonon interactions; E. Density functional theory

1. Introduction

CuAlO_2 has a delafossite structure (Left of Fig. 1) and a two-dimensional electronic structure caused by the natural super-lattices of O-Cu-O dumb-bell. Kawazoe *et al.* have found that the CuAlO_2 is p -type transparent conducting oxides (TCO) without any intentional doping. [1] Nakanishi *et al.* studied the pressure dependence of the structures [2] and the role of the self-interaction correction in CuAlO_2 . [3] Transparent p -type conductors such as CuAlO_2 are important for the p - n junction of TCO and a realization of high-efficiency photovoltaic solar-cells. First-principles calculations have shown the possibility for high efficiency thermoelectric power application with about 1% hole-doping. [4, 5, 6]

*Tel.: +81-6-6850-6504. Fax: +81-6-6850-6407.

Email address: nakanishi@aquarius.mp.es.osaka-u.ac.jp (Akitaka Nakanishi)

Katayama-Yoshida *et al.* have simulated the Fermi surface of the hole-doped CuAlO_2 by shifting the Fermi level rigidly and proposed that the nesting Fermi surface may cause a strong electron-phonon interaction thus a transparent superconductivity for visible light. [7] However, they have not calculated the superconducting transition temperature T_c . In previous study, we calculated the T_c of hole-doped CuAlO_2 [8] and found that the T_c increases up to about 50 K due to the strong electron-phonon interaction by the two dimensional flat valence band. The origin of the flat band is the π -band of hybridized O $2p_z$ and Cu $3d_{3z^2-r^2}$ on the frustrated triangular lattice in the two dimensional plane.

It is interesting to see the relation between the T_c and the flatness of the flat band by changing the Cu $3d_{3z^2-r^2}$, Ag $4d_{3z^2-r^2}$ and Au $5d_{3z^2-r^2}$. In the next study, we calculated the T_c of hole-doped delafossite AgAlO_2 and AuAlO_2 . [9] The calculated T_c are about 40 K for AgAlO_2 and 3 K for AuAlO_2 at maximum in the optimum hole-doping concentration. The low T_c of AuAlO_2 is attributed to the weak electron-phonon interaction caused by the low covalency and heavy atomic mass. In this study, we calculated T_c and the electron-phonon interaction versus the chemical trend of hole-doped CuBO_2 , CuAlO_2 , CuGaO_2 and CuInO_2 .

2. Calculation Methods

The calculations were performed within the density functional theory [10, 11] with a plane-wave pseudopotential method, as implemented in the Quantum-ESPRESSO code. [12] We employed the Perdew-Wang 91 [13] for CuBO_2 , CuAlO_2 and CuGaO_2 and the Perdew-Burke-Ernzerhof [14] for CuInO_2 generalized gradient approximation (GGA) exchange-correlation functional and ultra-soft pseudopotentials. [15] For the pseudopotentials, d electrons of transition metals were also included in the valence electrons. In reciprocal lattice space integral calculation, we used $8 \times 8 \times 8$ (electron and phonon) and $32 \times 32 \times 32$ (density of states and average at Fermi level) \mathbf{k} -point grids in the Monkhorst-Pack grid. [16] The energy cut-off for wave function was 40 Ry and that for charge density was 320 Ry. These \mathbf{k} -point grids and cut-off energies are fine enough to achieve convergence within 10 mRy/atom in the total energy.

The delafossite structure belongs to the space group $R\bar{3}m$ (No. 166) and is represented by cell parameters a and c , and internal parameter z (Left of Fig. 1). These parameters were optimized by the constant-pressure variable-cell

relaxation using the Parrinello-Rahman method [17] without any symmetry constraints.

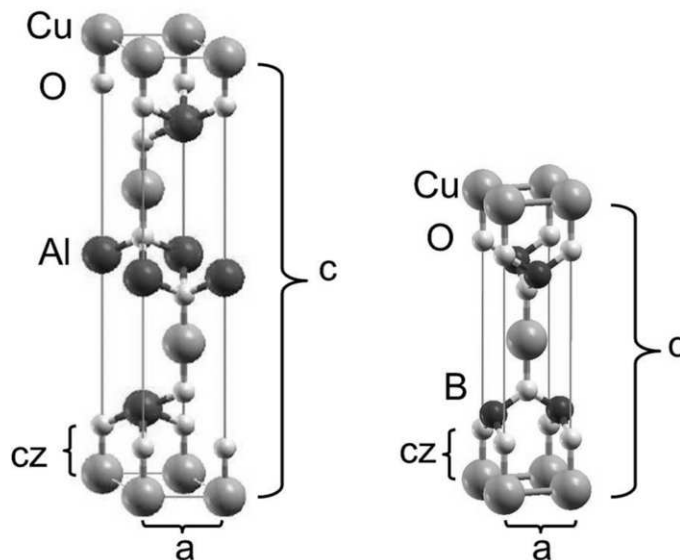


Figure 1: The crystal structure of delafossite CuAlO₂ (left) and body-centered tetragonal CuBO₂ (right).

As it is difficult for first-principles to exactly deal with doped systems, we had to implement some approximations. Let us take the electron-phonon interaction λ for example. λ is defined as follows:

$$\lambda = \sum_{\nu\mathbf{q}} \frac{2N(\varepsilon_F) \sum_{\mathbf{k}} |M_{\mathbf{k},\mathbf{k}+\mathbf{q}}^{\nu\mathbf{q}}|^2 \delta(\varepsilon_{\mathbf{k}} - \varepsilon_F) \delta(\varepsilon_{\mathbf{k}+\mathbf{q}} - \varepsilon_F)}{\omega_{\nu\mathbf{q}} \sum_{\mathbf{k}\mathbf{q}'} \delta(\varepsilon_{\mathbf{k}} - \varepsilon_F) \delta(\varepsilon_{\mathbf{k}+\mathbf{q}'} - \varepsilon_F)}. \quad (1)$$

(1) For the non-doped systems, we calculated the dynamical matrix, the phonon frequency $\omega_{\nu\mathbf{q}}$ and the electron-phonon matrix $M_{\mathbf{k},\mathbf{k}+\mathbf{q}}^{\nu\mathbf{q}}$. (2) For the doped systems, we calculated the Fermi level ε_F and the density of states at the Fermi level $N(\varepsilon_F)$ with the number of valence electrons reduced using the eigenvalues $\varepsilon_{\mathbf{k}}$ of the non-doped system. (3) By using the results of (1) and (2), we calculated the electron-phonon interaction λ and the other superconducting properties. This approximation is based on the idea that the doping does not greatly change electron and phonon band structures. In this study, we show the results of 0.1 \sim 1.0 hole-doped systems.

We calculated the superconducting transition temperature by using the Allen-Dynes modified McMillan formula. [18, 19] According to this formula, T_c is given by three parameters: the electron-phonon interaction λ , the logarithmic averaged phonon frequency ω_{\log} , and the screened Coulomb interaction μ^* , in the following form.

$$T_c = \frac{\omega_{\log}}{1.2} \exp\left(\frac{-1.04(1 + \lambda)}{\lambda - \mu^*(1 + 0.62\lambda)}\right). \quad (2)$$

$$\omega_{\log} = \exp\left(\frac{2}{\lambda} \int_0^\infty d\omega \frac{\alpha^2 F(\omega)}{\omega} \log \omega\right). \quad (3)$$

Here, $\alpha^2 F(\omega)$ is the Eliashberg function. λ and ω_{\log} are obtained by the first-principle calculations using the density functional perturbation theory. [20] As for μ^* , we assume the value $\mu^* = 0.1$. This value holds for weakly correlated materials.

3. Calculation Results and Discussion

First, we optimized the cell parameters. The results show that the optimized structure is delafossite as no structural transition occurred. However, the phonon frequency of CuBO_2 is negative. It means that the structure is only locally stable. Then after moving some atoms from their initial positions and optimizing the structure again, we found out that CuBO_2 relaxed to a body-centered tetragonal structure. This structure is represented by cell parameters a and c , and internal parameter z (Right of Fig. 1). Table 1 shows the optimized cell parameters.

	CuBO_2	CuAlO_2	CuGaO_2	CuInO_2
a [Å]	2.534	2.859	3.002	3.367
c/a	4.253	5.965	5.759	5.250
z	0.174	0.110	0.108	0.106

Table 1: The optimized cell parameters of body-centered tetragonal CuBO_2 and delafossite CuAlO_2 , CuGaO_2 and CuInO_2 .

Figures 2 and 3 show the band structures, the densities of states (DOS) and energy gaps. The energy gaps are 1.89 eV for CuBO_2 , 1.83 for CuAlO_2 , 0.82 for CuGaO_2 and 0.21 for CuInO_2 . Small gaps of CuGaO_2 and CuInO_2

show that these covalent bonding is weak. The target materials have the flat valence bands and small peaks of DOS due to the two dimensionality in O-Cu-O dumbbell array. These peaks are mainly constructed by the two-dimensional π -band of Cu $3d_{3z^2-r^2}$ -O $2p_z$ anti-bonding states. CuBO₂ has wider non-covalent Cu d -band and a narrower peak than CuAlO₂. This means that the covalency of CuBO₂ is lower than that of CuAlO₂ though their energy gaps are the same.

Figure 4 shows the electron-phonon interaction λ . There are peaks at the number of holes $N_h = 0.3$. In CuBO₂, a first peak is narrow and a second peak which is due to the narrow DOS peak appears in the heavily doped region of $N_h = 0.7 \sim 1.0$. CuAlO₂ has higher λ than CuBO₂, CuGaO₂ and CuInO₂. The difference in λ strength is due to the covalency mentioned above.

Figure 5 shows the logarithmic averaged phonon frequency ω_{\log} . These are almost constant for the number of holes. The difference of ω_{\log} is mainly due to atomic mass. Therefore, CuGaO₂ and CuInO₂ have smaller ω_{\log} than CuBO₂ and CuAlO₂. In the lightly doped region, CuBO₂ and CuAlO₂ have almost the same ω_{\log} though Al is heavier than B. This is due to large electron-phonon interaction of CuAlO₂.

Figure 6 shows the superconducting transition temperature T_c . Since CuInO₂ has very low T_c ($< 1 K$), its curve is no longer invisible in Fig. 6. The T_c variation is determined mainly by the electron-phonon interaction because logarithmic averaged phonon frequencies ω_{\log} are almost constant for the number of holes. CuBO₂, CuGaO₂ and CuInO₂ have much lower T_c than CuAlO₂ because they have low covalency and λ as mentioned above.

4. Conclusions

In summary, we calculated the chemical trend of superconducting transition temperature of the hole-doped delafossite CuBO₂, CuAlO₂, CuGaO₂ and CuInO₂. The calculated T_c are about 50 K for CuAlO₂, 10 K for CuBO₂ and CuGaO₂ and 1 K for CuInO₂ at maximum in the optimum hole-doping concentration. The low T_c of CuInO₂ is attributed to the weak electron-phonon interaction caused by the low covalency and heavy atomic mass.

Acknowledgment

The authors acknowledge the financial support from the Global Center of Excellence (COE) program "Core Research and Engineering of Advanced

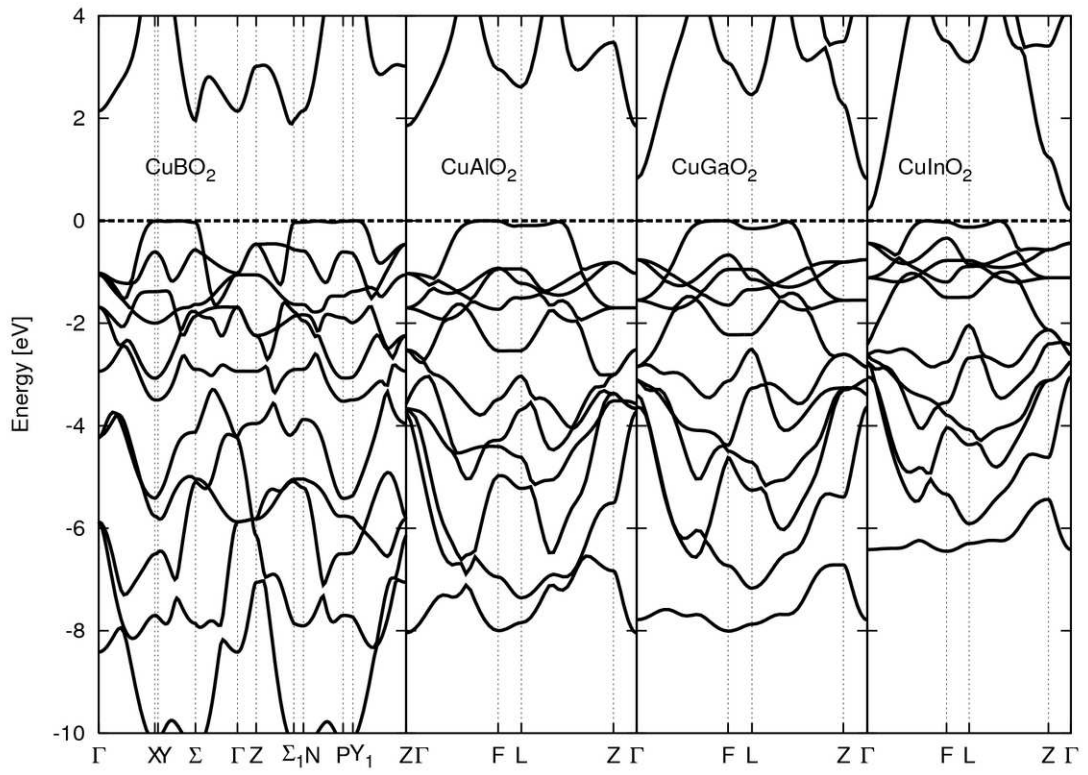


Figure 2: Band structures of CuBO₂, CuAlO₂, CuGaO₂ and CuInO₂.

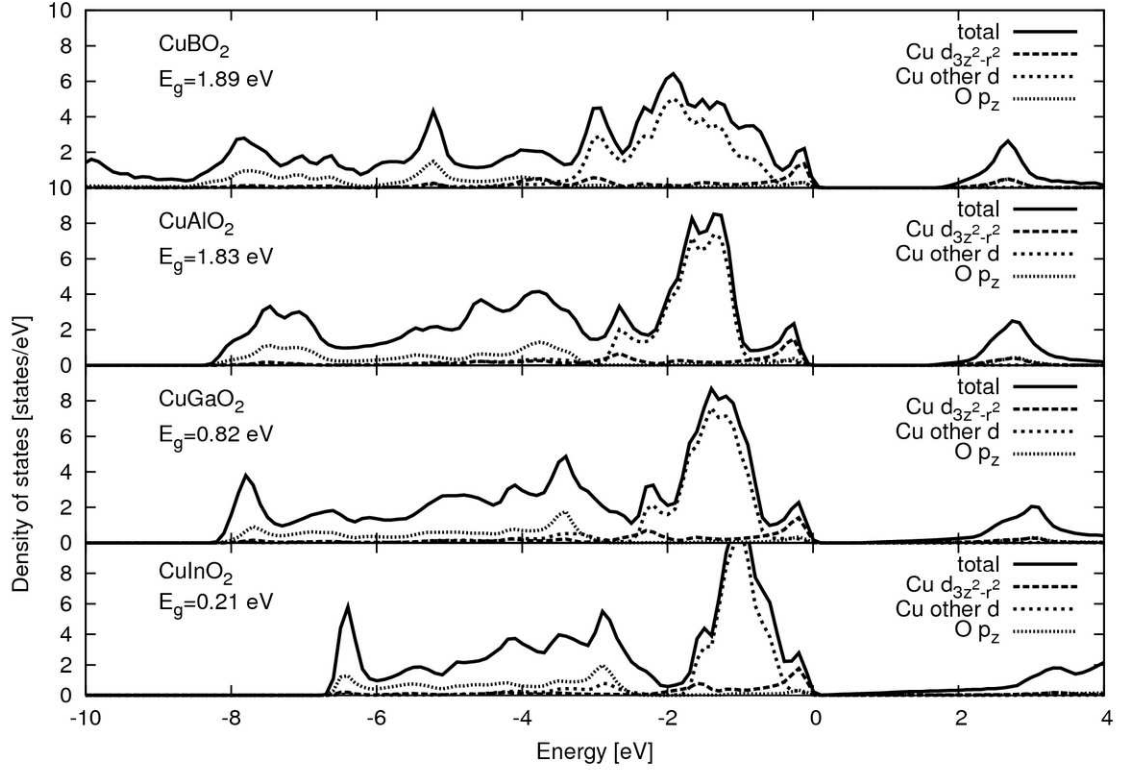


Figure 3: Density of states and energy gaps.

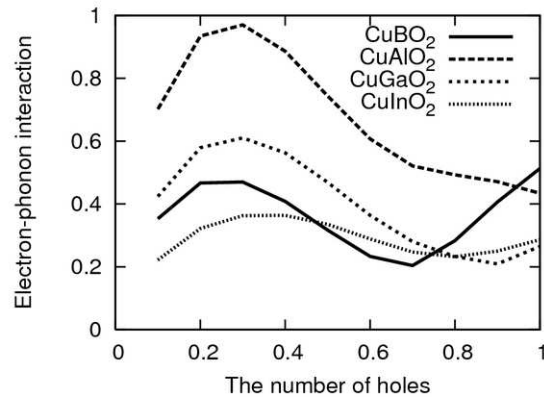


Figure 4: Electron-phonon interaction λ .

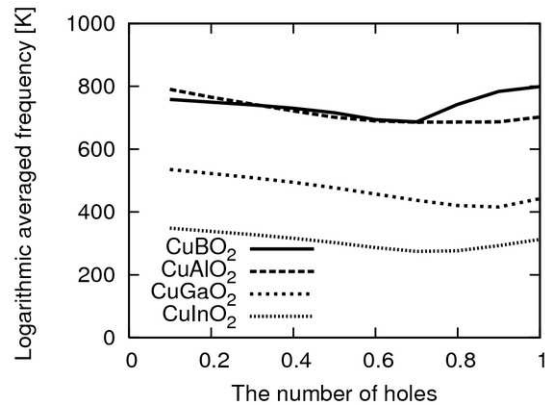


Figure 5: Logarithmic averaged phonon frequency ω_{\log} .

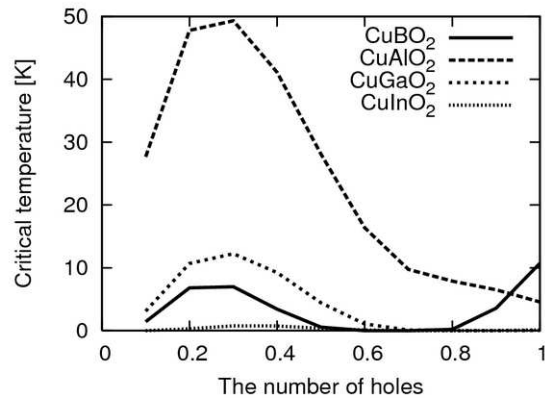


Figure 6: Superconducting transition temperature T_c .

Materials - Interdisciplinary Education Center for Materials Science”, the Ministry of Education, Culture, Sports, Science and Technology, Japan, and a Grant-in-Aid for Scientific Research on Innovative Areas ”Materials Design through Computics: Correlation and Non-Equilibrium Dynamics”. We also thank to the financial support from the Advanced Low Carbon Technology Research and Development Program, the Japan Science and Technology Agency for the financial support.

References

- [1] H. Kawazoe, M. Yasukawa, H. Hyodo, M. Kurita, H. Yanagi, H. Hosono, *Nature* 389 (1997) 939.
- [2] A. Nakanishi, H. Katayama-Yoshida, *J. Phys. Soc. Jpn.* 80 (2011) 024706.
- [3] A. Nakanishi, H. Katayama-Yoshida, *J. Phys. Soc. Jpn.* 80 (2011) 053706.
- [4] H. Funashima, A. Yanase, H. Harima, H. Katayama-Yoshida, *Proceedings of 23rd International Conference on Thermoelectrics (2004)* 237–238.
- [5] H. Katayama-Yoshida, H. Funashima, I. Hamada, H. Harima, A. Yanase, *Fabrication method and high-efficient thermo-electric power materials by two-dimensional natural super-lattices of CuAlO_2* , Japan Patent 652696 (2009).
- [6] I. Hamada, H. Katayama-Yoshida, *Physica B* 376 (2006) 808.
- [7] H. Katayama-Yoshida, T. Koyanagi, H. Funashima, H. Harima, A. Yanase, *Solid State Communication* 126 (2003) 135.
- [8] A. Nakanishi, H. Katayama-Yoshida, *Solid State Communication* 152 (2012) 24.
- [9] A. Nakanishi, H. Katayama-Yoshida, *Solid State Communication* 152 (2012) 2078–2081.
- [10] P. Hohenberg, W. Kohn, *Phys. Rev.* 136 (1964) B864.

- [11] W. Kohn, L. J. Sham, *Phys. Rev.* 140 (1965) A1133.
- [12] P. Giannozzi, S. Baroni, N. Bonini, M. Calandra, R. Car, C. Cavazzoni, D. Ceresoli, G. L. Chiarotti, M. Cococcioni, I. Dabo, A. D. Corso, S. Fabris, G. Fratesi, S. de Gironcoli, R. Gebauer, U. Gerstmann, C. Gougousis, A. Kokalj, M. Lazzeri, L. Martin-Samos, N. Marzari, F. Mauri, R. Mazzarello, S. Paolini, A. Pasquarello, L. Paulatto, C. Sbraccia, S. Scandolo, G. Sclauzero, A. P. Seitsonen, A. Smogunov, P. Umari, R. M. Wentzcovitch, *J. Phys.:Condens. Matter* 21 (2009) 395502.
- [13] *Phys. Rev. B* 46 (1992) 6671.
- [14] J. P. Perdew, K. Burke, M. Ernzerhof, *Phys. Rev. Lett.* 77 (1996) 3865.
- [15] D. Vanderbilt, *Phys. Rev. B* 41 (1990) 7892.
- [16] H. J. Monkhorst, J. D. Pack, *Phys. Rev. B* 13 (1976) 5188.
- [17] M. Parrinello, A. Rahman, *Phys. Rev. Lett.* 45 (1980) 1196.
- [18] W. L. McMillan, *Phys. Rev.* 167 (1968) 331.
- [19] P. B. Allen, R. C. Dynes, *Phys. Rev. B* 12 (1975) 905.
- [20] S. Baroni, S. de Gironcoli, A. D. Corso, P. Giannozzi, *Rev. Mod. Phys.* 731 (2001) 515.